

Observation of the Formation of an Optical Intensity Shock and Wave Breaking in the Nonlinear Propagation of Pulses in Optical Fibers

Joshua E. Rothenberg and D. Grischkowsky

IBM Thomas J. Watson Research Center, P.O. Box 218, Yorktown Heights, New York 10598

(Received 11 October 1988)

We have observed the formation of an optical intensity shock and the subsequent wave breaking in the nonlinear propagation of 1-psec pulses in an optical fiber. The wave breaking manifests itself as the appearance of oscillations trailing the shock, which are due to the beating of widely separated frequency components which bridge the shock. The experimental results are in good agreement with numerical solutions of the nonlinear Schrödinger equation.

PACS numbers: 41.10.-j, 42.10.-s, 42.81.-i

Nonlinear wave propagation has received much attention recently, both because it is rich in unique phenomena relevant to many physical systems and because the theoretical treatment involves a high degree of mathematical sophistication and challenge.¹ In this class of problems the nonlinear Schrödinger equation (NLSE) is of fundamental importance because it represents the general situation of dispersive wave propagation with a weak nonlinearity.² Optical propagation in single-mode fibers provides an excellent physical system for study of the NLSE because the single-mode propagation allows the problem to be reduced to the equivalent 1D (plane) wave propagation problem, and because the fibers have extremely low loss. The NLSE includes two physical effects, group-velocity dispersion (GVD) and self-phase modulation (SPM) due to the intensity-dependent refractive index. Depending on their relative signs, they combine to allow bright solitary waves,³⁻⁵ or (in the visible region of optical fibers) dark solitary waves,^{3,4,6,7} enhanced frequency chirping,⁸ and "optical wave breaking."⁹

A prominent class of phenomena in nonlinear wave propagation is that of shocks and breaking,¹ which are known to occur in many diverse physical systems. Breaking, a phenomenon inseparable from shocks, occurs when the top of the shock overtakes the bottom, similar to the breaking of water waves.^{1,9} The possibility of so-called optical intensity "envelope" shocks was first theoretically suggested by several researchers^{10,11} some twenty years ago. In the descriptions of Ref. 10, a higher-order nonlinear term was considered which results in an intensity-dependent group velocity, but because they ignored the effects of dispersion, the shock formation proposed there has never been observed. Although, for optical pulses propagating in strongly nonlinear, dispersive near-resonant vapors, nsec observations of self-steepening have been reported.¹² In addition, Hasegawa and Tappert⁴ have pointed out that the dark pulse solitary wave is, in fact, an example in the class of envelope shocks proposed by Ostrovskii.¹¹

In this Letter we describe the first high-resolution (0.1

psec) measurements of the formation of an intensity (envelope) shock and the subsequent oscillations due to wave breaking. We measured the reshaped output pulse from a 250-cm single-mode optical fiber versus the power of a 1-psec input pulse. Over a wide range of input powers, the output pulse has remarkably sharp self-steepened shocks of less than 0.2-psec duration. At a critical peak power of 250 W, well-defined 0.3-psec oscillations due to optical wave breaking begin to develop adjacent to the shocks.

Previous measurements of nonlinear visible pulse propagation in single-mode fibers established the characteristic rectangular reshaping and enhanced frequency chirping of the output pulses.⁸ There and in subsequent numerical calculations^{9,13,14} it was found that the combined effects of SPM and GVD resulted in the following pulse-shape evolution during propagation through a nonlinear fiber. Initially, pulse-intensity reshaping is minimal and all that occurs is simple SPM, where the central portion of the pulse develops a positive frequency sweep and the edges develop negative sweeps. As the pulse propagates further, the positive sweep stretches under the influence of normal GVD, but the edges compress. The result is a broadening rectangular pulse of positive frequency sweep with increasingly sharp edges which have accordingly more rapid frequency transitions from their maximum frequency shifts back to the carrier. At a critical distance, the negative frequency sweep and the edges go through a singularity, indicating the formation of the shocks. Subsequently, the edges of the rectangular pulse overlap (break) the wings of the pulse and the resulting interference between the shifted frequency components and the carrier frequency causes oscillations to appear on the wings of the pulse. This phenomenon was first termed "optical wave breaking" by Tomlinson, Stolen and Johnson.⁹ Their high-resolution numerical calculations showed these oscillations in detail and explained the accompanying change in the power spectra observed in fiber-transmission experiments.¹⁵ There have been a few attempts to observe this effect with streak cameras, both in the spectral and in the time

domain.¹⁶⁻¹⁸ Nelson *et al.*¹⁶ observed the intensity time dependence, and Gomes, Gouveia-Neto, and Taylor¹⁷ and Hamaide and Emplit¹⁸ observed the spectral time dependence. In these cases the temporal resolution was insufficient to observe the predicted intensity oscillations of wave breaking.

To understand why this observation has eluded workers in the past, consider the experimental configuration of Fig. 1. A synchronously pumped, cavity-dumped dye laser with an intracavity saturable absorber supplies 608-nm, 1-psec pulses at a repetition rate of 4 MHz. The output beam is split and focused into two separate polarization-preserving fibers with core diameters of 4 μm . One fiber is 60 cm long and after compression of the output through a grating pair we obtain 120-fsec probe pulses. The other fiber is 250 cm long and its output (signal) pulse is the subject of our investigation. In the simplest configuration (shown in the dashed box of Fig. 1), one samples the signal pulse with the probe pulse in a noncollinear cross-correlation arrangement,⁸ where the beams cross at their focus in a 0.3-mm LiIO_3 crystal. The delay of the probe beam is varied and the second harmonic is detected with a photomultiplier tube (PMT) and recorded. Unfortunately, observation of the very fast signal-pulse edge is difficult because its time position is extremely sensitive to the dye-laser input pulse power, shape, and frequency. For example, since the signal-pulse width is approximately proportional to the input pulse power, a power stability of better than 5% is required to observe an edge with a resolution of 120 fsec. Probably even more critical is the input pulse-shape stability. Consequently, this standard cross-correlation technique yielded none of the fast features predicted.

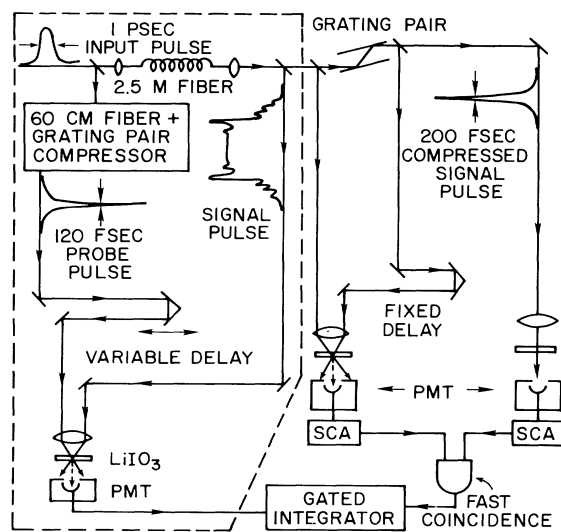


FIG. 1. Schematic of experimental arrangement, with the standard cross correlator inside the dashed box, and the pulse selection apparatus outside.

To overcome this stability problem, we use one of the sharp pulse edges (either leading or trailing) as a criterion to select and sample only those output pulses whose edges occur at a specified time. This effectively locks the time position of that edge. This is accomplished by taking a portion of the signal output pulse and cross correlating it with another portion of the signal pulse which has been compressed by a (second) grating pair. This second cross correlator is set with a *fixed* delay corresponding to the 50% point of either edge of the pulse, and the output of its PMT is selected to be within a certain range by a single-channel analyzer. The signal was further improved by simultaneous restriction of the peak power of the compressed signal pulse by detection of the second harmonic it generates with a PMT connected to a second single-channel analyzer. The outputs of the two single-channel analyzers drove a fast coincidence detector, which triggered a gated integrator. The gated integrator sampled the PMT of the (first) signal cross correlator which was scanned (typically ten times) and thus measured the intensity profile of only those pulses meeting both selection criteria. These coincident sampling rates were only 1–10 kHz compared to the optical pulse rate of 4 MHz. In the following measurements of the trailing edge of the pulse, we have selected on that edge; similar results are found for the leading edge when it is selected upon.

In Fig. 2 we show a measured sequence of the input pulse [Fig. 2(a)] and output pulses together with the corresponding numerical calculations, for increasing input-pulse peak power. At 125 W [Fig. 2(b)], the observed output pulse has broadened to a rectangularlike pulse with a sharp ~ 300 -fsec trailing edge. The observed asymmetry is not completely understood; however, when the selection is set on the leading edge of the pulse, it sharpens up just as the trailing edge. In addition, phase modulation of the input pulse, whose spectrum is about twice the transform limit, may be contributing to the asymmetry. As the power is further increased, our observations concentrated on the development of the trailing edge of the rectangular pulse. At 250 W [Fig. 2(c)], shown on a higher-resolution time scale, the trailing edge has steepened to a ~ 200 -fsec shock (80% to 20% fall time) and oscillations are just appearing, indicating the onset of wave breaking. In Fig. 2(d), at 500 W, wave breaking is clearly seen; the oscillations are prominent both before and after the shock, which has steepened to ~ 160 fsec. The ~ 300 -fsec period of the trailing oscillations corresponds to a frequency difference of $\sim 100 \text{ cm}^{-1}$, which is consistent with the observed spectrum. We note a striking similarity between these data and those obtained in shock formation in plasmas.¹⁹ At the still higher power of 750 W [Fig. 2(e)], the shock steepened no further, indicating that we reached our resolution limit, while the contrast of the oscillations decreased as they formed an increasingly larger trailing

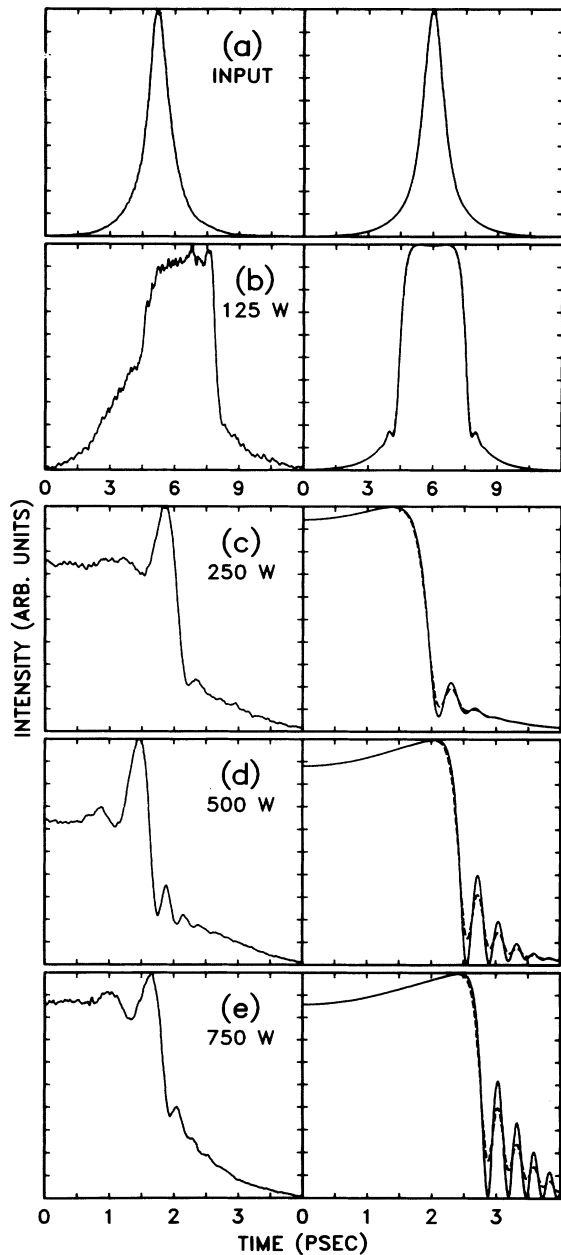


FIG. 2. Observed (first column) and calculated pulse intensities (second column), solid curves. (a) input pulse; (b)–(e) output pulse for indicated input pulse peak powers. Dashed curves are blurred with 120-fsec sech^2 resolution function.

wing.

The numerical integrations of the NLSE use an implicit centered difference method with an input pulse obtained from a fit [Fig. 2(a)] to the measured input pulse assuming no phase modulation and the indicated peak intensities. Because the calculations give a symmetric output pulse as shown in Fig. 2(b), we show only the trailing half of the calculated pulse in Figs. 2(c)–2(e).

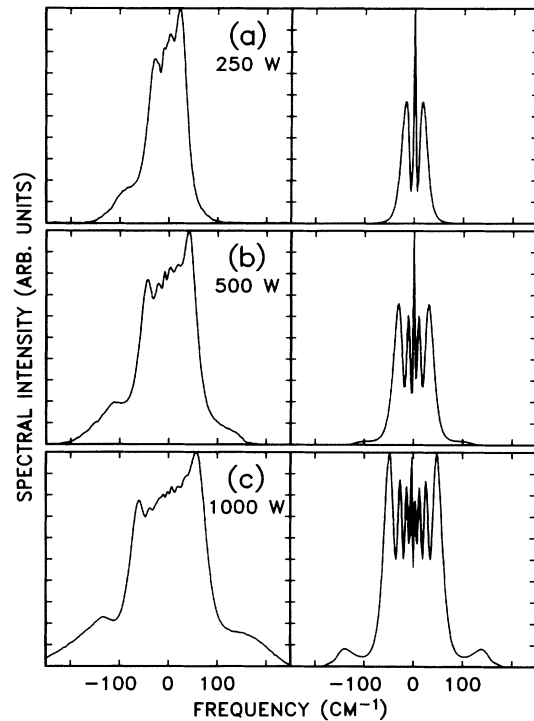


FIG. 3. Observed (first column) and calculated output pulse spectra (second column) for indicated input peak powers.

At 250 W [Fig. 2(c)], the calculation shows a ~ 250 -fsec pulse edge and the onset of oscillations as the shock is just forming. For 500 and 750 W [Figs. 2(d) and 2(e)], the shock has steepened to 150 and 130 fsec, respectively, and wave breaking is clearly seen as indicated by the 330-fsec oscillations. For comparison with the data, these calculations are cross correlated with a sech^2 probing pulse of 120 fsec FWHM (dashed curves). It appears from the data that our resolution is slightly poorer than the probe width of 120 fsec, which is indicative of residual timing jitter in our selection technique.

The measured spectra (4 cm^{-1} resolution) and calculations are shown near the onset of wave breaking in Fig. 3. Here one should focus on the high-frequency side, since this corresponds to the trailing pulse edge. The sharp high-frequency edge in Fig. 3(a) shows the spectrum at the formation of the optical shock and before significant wave breaking has occurred (note the absence of any satellite on the high-frequency side). The satellite on the low-frequency side is not predicted by the calculations and is most likely due to stimulated Raman scattering. As the power is increased, we see a broadening of the spectrum and then, commensurate with the development of the intensity oscillations, we observe the formation of satellites¹⁵ [Figs. 3(b) and 3(c)], which, on the high-frequency side, are in good agreement with the calculations. It should be noted that once the SPM nonlinearity has set up the negative frequency sweeps in the

pulse, subsequent linear propagation will lead to breaking that is very similar to what has been observed here. However, in the linear case, although intensity oscillations appear, no spectral satellites are formed. These satellites are the result of nonlinear mixing of the overlapping frequencies to create new frequencies at \pm the frequency difference.⁹ This mixing process is related to "modulation instability" as has been noted by Agrawal.²⁰

In general, our calculations are in good qualitative agreement with our observations and verify that indeed the optical intensity shock and wave breaking have been observed. However, a departure from our own and previous calculations^{8,9,13} is the appearance of oscillations and a peak immediately before the shock. Although Lassen *et al.*¹⁴ have found peaks in their NLSE solutions for very lossy fibers, the linear loss of our fiber is too small to be responsible for the observed peak. Therefore, the addition of higher-order terms to the NLSE may be indicated.²¹ The inclusion of the nonlinear group-velocity term mentioned earlier is about a factor of 10 too small to have any significant effect at our power levels. However, Raman scattering has led to some important effects at these power levels in soliton experiments,²² and appears to have affected our spectral data. Therefore, its investigation in the normal dispersion regime may be warranted.

This work was supported in part by the U.S. Office of Naval Research.

¹G. B. Whitham, *Linear and Nonlinear Waves* (Wiley, New York, 1974).

²H. C. Yuen and B. M. Lake, in *Solitons in Action*, edited by K. Lonngren and A. Scott (Academic, New York, 1978).

³V. E. Zakarov and A. B. Shabat, *Zh. Eksp. Teor. Fiz.* **61**,

118 (1971), and **64**, 1627 (1973) [*Sov. Phys. JETP* **34**, 62 (1972), and **37**, 823 (1973)].

⁴A. Hasegawa and F. Tappert, *Appl. Phys. Lett.* **23**, 142, 171 (1973).

⁵L. F. Mollenauer, R. H. Stolen, and J. P. Gordon, *Phys. Rev. Lett.* **45**, 1095 (1980).

⁶P. Emplit, J. P. Hamaide, F. Reynaud, C. Froehly, and A. Barthelemy, *Opt. Commun.* **62**, 374 (1987).

⁷D. Krokkel, N. J. Halas, G. Giuliani, and D. Grischkowsky, *Phys. Rev. Lett.* **60**, 29 (1988).

⁸H. Nakatsuka, D. Grischkowsky, and A. C. Balant, *Phys. Rev. Lett.* **47**, 910 (1981); D. Grischkowsky and A. C. Balant, *Appl. Phys. Lett.* **41**, 1 (1982).

⁹W. J. Tomlinson, R. H. Stolen, and A. M. Johnson, *Opt. Lett.* **10**, 457 (1985).

¹⁰R. J. Joenk and R. Landauer, *Phys. Lett.* **24A**, 228 (1967); F. DeMartini, C. H. Townes, T. K. Gustafson, and P. L. Kelley, *Phys. Rev.* **164**, 312 (1967).

¹¹L. A. Ostrovskii, *Zh. Eksp. Teor. Fiz.* **54**, 1235 (1968) [*Sov. Phys. JETP* **27**, 660 (1968)].

¹²D. Grischkowsky, E. Courtens, and J. A. Armstrong, *Phys. Rev. Lett.* **31**, 422 (1973).

¹³W. J. Tomlinson, R. H. Stolen, and C. V. Shank, *J. Opt. Soc. Am. B* **1**, 139 (1984).

¹⁴H. E. Lassen, F. Mengel, B. Tromborg, N. C. Albertsen, and P. L. Christiansen, *Opt. Lett.* **10**, 34 (1985).

¹⁵A. M. Johnson and W. M. Simpson, *J. Opt. Soc. Am. B* **2**, 619 (1985).

¹⁶B. P. Nelson, D. Cotter, K. J. Blow, and N. J. Doran, *Opt. Commun.* **48**, 292 (1983).

¹⁷A. S. L. Gomes, A. S. Gouveia-Neto, and J. R. Taylor, *Electron. Lett.* **22**, 41 (1986).

¹⁸J.-P. Hamaide and P. Emplit, *Electron. Lett.* **24**, 818 (1988).

¹⁹K. Saeki, *J. Phys. Soc. Jpn.* **35**, 251 (1973).

²⁰G. P. Agrawal, *Phys. Rev. Lett.* **59**, 880 (1987).

²¹E. Bourkoff, W. Zhao, R. I. Joseph, and D. N. Christodoulides, *Opt. Lett.* **12**, 272 (1987).

²²F. M. Mitschke and L. F. Mollenauer, *Opt. Lett.* **11**, 659 (1986).